



Exchange biased FeNi/FeMn bilayers with coercivity and switching field enhanced by FeMn surface oxidation

A. V. Svalov, P. A. Savin, V. N. Lepalovskij, A. Larrañaga, V. O. Vas'kovskiy, A. Garcia Arribas, and G. V. Kuryandskaya

Citation: *AIP Advances* **3**, 092104 (2013); doi: 10.1063/1.4821105

View online: <http://dx.doi.org/10.1063/1.4821105>

View Table of Contents: <http://scitation.aip.org/content/aip/journal/adva/3/9?ver=pdfcov>

Published by the *AIP Publishing*

Articles you may be interested in

[Asymmetric recovery effect of exchange bias in polycrystalline NiFe/FeMn bilayers](#)

J. Appl. Phys. **106**, 063903 (2009); 10.1063/1.3211314

[Exchange bias, training effect, hysteretic behavior of angular dependence, and rotational hysteresis loss in NiFe/FeMn bilayer: Effect of antiferromagnet layer thickness](#)

J. Appl. Phys. **105**, 053913 (2009); 10.1063/1.3087450

[Thermal stability of exchange bias in FeMn based bilayers](#)

J. Appl. Phys. **91**, 5272 (2002); 10.1063/1.1446661

[Magnetization reversal in the pinned layer of PtMnCr/NiFe exchange biased bilayers](#)

J. Appl. Phys. **89**, 6591 (2001); 10.1063/1.1359793

[Exchange-biased magnetic tunnel junctions fabricated with in situ natural oxidation](#)

J. Appl. Phys. **85**, 5261 (1999); 10.1063/1.369960



Exchange biased FeNi/FeMn bilayers with coercivity and switching field enhanced by FeMn surface oxidation

A. V. Svalov,^{1,2} P. A. Savin,² V. N. Lepalovskij,² A. Larrañaga,³
 V. O. Vas'kovskiy,² A. Garcia Arribas,^{1,4} and G. V. Kuryandanskaya^{1,2,a}

¹*Departamento de Electricidad y Electrónica, Universidad del País Vasco (UPV/EHU),
 48080 Bilbao, Spain*

²*Department of Magnetism and Magnetic Nanomaterials, Ural Federal University,
 620002 Ekaterinburg, Russia*

³*SGIker, Servicios Generales de Investigación, Universidad del País Vasco,
 48080 Bilbao, Spain*

⁴*BCMaterials, Universidad del País Vasco (UPV/EHU), 48080 Bilbao, Spain*

(Received 16 June 2013; accepted 28 August 2013; published online 5 September 2013)

FeNi/FeMn bilayers were grown in a magnetic field and subjected to heat treatments at temperatures of 50 to 350 °C in vacuum or in a gas mixture containing oxygen. In the as-deposited state, the hysteresis loop of 30 nm FeNi layer was shifted. Low temperature annealing leads to a decrease of the exchange bias field. Heat treatments at higher temperatures in gas mixture result in partial oxidation of 20 nm thick FeMn layer leading to a nonlinear dependence of coercivity and a switching field of FeNi layer on annealing temperature. The maximum of coercivity and switching field were observed after annealing at 300 °C. © 2013 Author(s). All article content, except where otherwise noted, is licensed under a Creative Commons Attribution 3.0 Unported License. [<http://dx.doi.org/10.1063/1.4821105>]

I. INTRODUCTION

Spin-valve layered structures are the base for many magnetic field sensors and other magneto-electronic devices.¹ Their principle of operation is based on the phenomenon of giant magnetoresistance, which can be observed as a result of a change of the relative orientation of the magnetizations in adjacent layers.² The simplest spin-valve structures consist of two magnetic layers. The first one is a magnetically soft ferromagnetic layer (FM) with a magnetization easily rotating by the external magnetic field. The second FM layer is separated from the first one by a layer of non-magnetic metal. The magnetization of the second FM layer should remain non-affected by the external field. It can be obtained in the case of different coercivities of adjacent magnetic layers (so-called hard-soft systems), in the case of pinning the magnetization of FM layers by the exchange bias interaction with the third (antiferromagnetic or ferrimagnetic) layer² or by the exchange bias with multilayer structures (artificial antiferromagnetic or ferrimagnetic).^{3,4} The hysteresis loop of an exchange biased FM layer is shifted with respect to zero field, this enables the moment of other FM layers in a heterostructure to be switched without affecting the magnetic state of the biased layer.

For practical applications antiferromagnetic (AFM) layers are often used,⁵ and the most popular material remains FeMn.^{2,3} In general, bias is often set by field cooling the bilayer through the blocking temperature T_B , but in the case of FeMn it can be achieved simply by depositing the FeMn layer onto a FM saturated layer.⁵ One disadvantage of FeMn films is their increased oxidation ability, especially for manganese.⁶ Strong oxidation leads to degradation of antiferromagnetic properties of FeMn layer and disappearance of the exchange bias of adjacent FM layer. However, partial surface oxidation of Mn results in a decrease of the effective thickness of the FeMn layer and provokes Mn migration to the surface, creating inside the FeMn layer a region with ferromagnetic properties enriched in

^aElectronic mail: galina@we.lc.ehu.es



Fe.⁷ Although details of the process of oxidation of FeMn films have been widely discussed in the literature,^{6–8} the impact of this process on the properties of exchange biased FeNi/FeMn bilayers has been far less investigated. This problem is all the more important, because the probability of partial oxidation FeMn layer increases with increasing temperature. The temperature increase is inevitable for many standard processing techniques of sensor fabrication.^{9,10} Although high switching fields and post-deposition annealing treatments have already been achieved in MRAM (magnetoresistive random-access memory) devices (see an example for ferromagnetic storage CoFe(2 nm)/FeNi(3 nm) electrode)¹¹ and in particular on thermally assisted MRAMs, different physical processes can be involved in the exchange bias field changes. It is also worse to mention that the thickness of FeNi biased film is a very important parameter for a number of technological applications.

In this work, we studied magnetic properties of exchange biased FeNi(30 nm)/FeMn(20 nm) bilayers prepared by magnetron sputtering and annealed in vacuum or in gas mixtures containing oxygen in order to gain insight on the influence of partial oxidation of FeMn layer on the exchange bias strength, coercivity and switching field of these bilayers.

II. METHODS

The FeNi(30 nm)/FeMn(20 nm) samples were deposited by magnetron sputtering at room temperature onto glass substrates with a 5-nm-thick Ta underlayer. The background pressure was 3×10^{-7} mbar. Deposition was performed in an Ar atmosphere with 2×10^{-3} mbar pressure. Permalloy was sputtered using a Fe₁₉Ni₈₁ target and an antiferromagnetic layer using Fe₅₀Mn₅₀ target. The tantalum underlayer was incorporated in order to promote a (111) texture in FeNi and FeMn layers. One part of the samples was capped by a 10-nm-thick Ta layer aiming to reduce the possibility of oxidation of the magnetic layers. The other part of the samples was prepared without Ta capping layer. The deposition rates were previously calibrated as 8 nm/min for FeNi layers, 5 nm/min for FeMn layers and 2 nm/min for Ta layers. A magnetic field of about 250 Oe was applied during the sample preparation parallel to the substrate surface to induce a uniaxial anisotropy and the exchange bias. Annealing was carried out at temperatures of 50 to 350 °C in vacuum or in a mixture of N₂ + 0.5% O₂ for exposure time up to 1 h in a magnetic field of 300 Oe applied along the same direction as during the film deposition. The heating and cooling rates were set to 20 K/min. The samples with a tantalum protective layer were subjected to heat treatment in vacuum (samples type I). This was done in order to further insure protection against possible FeMn layer oxidation. On the contrary, the samples without a protective layer were annealed in the gas mixture (samples type II). The microstructure was studied by X-ray diffraction (XRD) using Cu-*K*α radiation. The hysteresis loops were measured using a vibrating-sample magnetometer (VSM).

The samples of both types on the as-deposited state revealed an antiferromagnetic FeMn γ -phase with (111) preferred orientation. The Ta underlayer enhanced the (111) orientation of the FeNi film which resulted in the growth of the FeMn layer into well oriented (111) γ -phase.

III. RESULTS AND DISCUSSION

For all as-deposited sample the VSM loop was characterized by a bias field, $H_E = 30$ Oe, a coercive field, $H_C = 3$ Oe. A blocking temperature, $T_b \approx 140$ °C. The annealing (post-deposition heat treatment) up to 200 °C of both types of samples leads to a double reduction H_E and a twofold increase in H_C (Fig. 1). Such a reduction in H_E in low-temperature annealing is a fairly common phenomenon.^{12–15} The cause of this reduction might be a strain relief in the crystal structure or movement of impurities from the interior of grains to the grain boundaries. Both phenomena have an impact on the state of inter-layer interface, which, in turn, determines an exchange coupling across the interface between the FeNi and FeMn spins. Note also that in order to create the requested H_E one can heat the sample above T_b and then cool it in a magnetic field.⁵ In our case such a procedure did not result in the obtaining of the H_E values above the H_E corresponding to as-deposited state. Perhaps it is a confirmation of the previously expressed hypothesis that the deposition of the films in applied field and post-deposition heating/cooling of the samples in magnetic field have a different

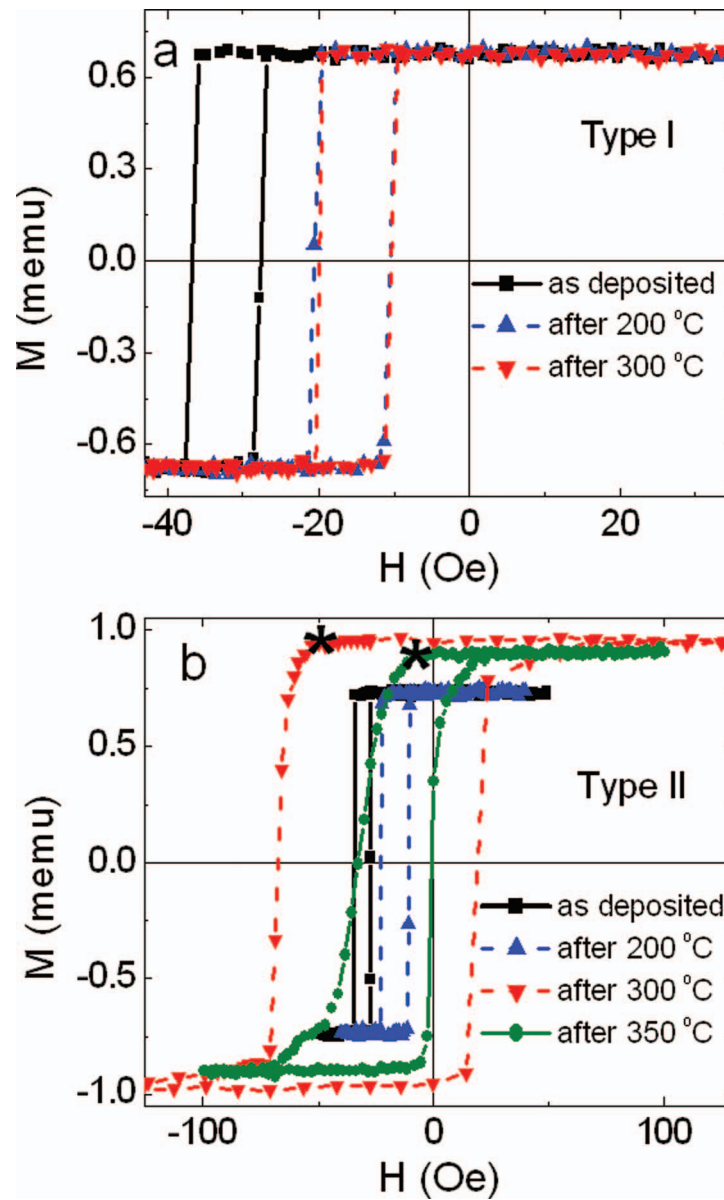


FIG. 1. $M(H)$ loops of the type I (a) and type II (b) samples measured for as-deposited state and after annealing at different temperatures. Annealing time is 5 min.

effect on the exchange bias fields due to different responsible physical processes^{16,17} like thermal activation energies and diffusion rates.

Annealing at higher temperatures does not appreciably alter the magnetic properties of the type I samples. The magnetic moment of these samples is determined by the FeNi layer. The estimation of the magnetization of the FeNi layer gives us the expected value of 800 emu/cm^3 . For type II samples, on the contrary, annealing at temperatures above 250°C leads to a sharp increase in H_c with a peak roughly around 300°C . Afterwards there is a drastic decline in H_c . With regard to H_E , it varies slightly. Fig. 2 summarizes the change in the H_E and H_c of type I and type II samples with different annealing temperatures. In addition, the same figure shows the dependence of the switching field in the direction opposite to the pinned direction, H_{sw} . For samples type I, characterized by square shape of the hysteresis loop, $H_{sw} = H_E + H_c$. For samples type II the high temperature annealing leads to a change of the shape of the hysteresis loop: it becomes tilted. Therefore we have taken the

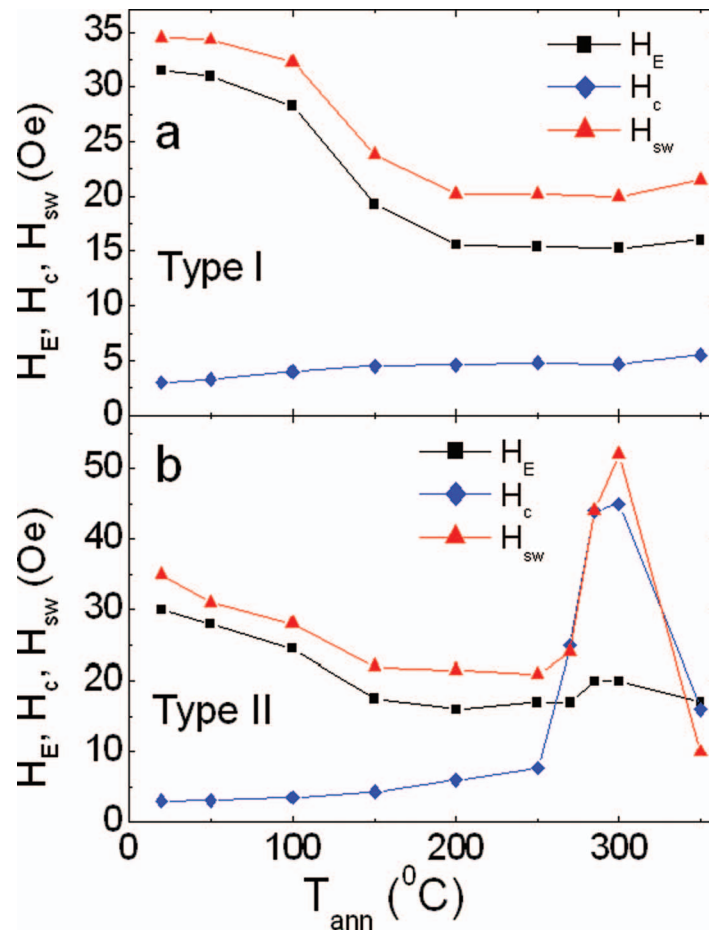


FIG. 2. Exchange bias, coercivity and switching field for type I (a) and type II (b) samples as a function of the annealing temperature. Annealing time is 5 min.

H_{SW} value as the field in the second quadrant of the loop from which the decrease of the magnetic moment began (indicated by asterisks, Fig. 1(b)).

In addition, the high temperature annealing of type II samples resulted in a growth of the magnetic moment of the samples (Fig. 1(b)). It is logical to suppose that the increase of the magnetic moment is due to partial oxidation of Mn in the layer and the formation inside the FeMn layer of a region which is Fe rich and Mn depleted as compared to the initial composition of the film. Most probably it happens near the grain boundaries. It is known that the preferential oxidation of Mn at the surface leads to the formation a surface oxide layer, which is Mn-rich, and drives Mn migration from deeper film region, leaving it Fe-rich.^{7,18} The magnetization for Fe-rich phase⁷ can reach 1200–1400 emu/cm³.

Fig. 3 shows the X-ray diffraction patterns of type II samples in the as-deposited state and after annealing at 300 $^{\circ}\text{C}$ (5 min). Annealing barely affects the intensity of FeNi (111) peak, but results in the disappearance of the γ -FeMn peak. At the same time MnO (111) peak appears (inset Fig. 3), in this case it does not appear in the diffraction patterns for type I samples. The absence of other lines corresponding to the oxide of manganese seems logical because (111) texture of the FeMn layer may specify a similar texture and in MnO. Strictly speaking, the diffraction peak at about 35.5 $^{\circ}$ may be caused by the presence of iron oxides. The lines of Mn and Fe oxides are very close to each other and they cannot be identified precisely in this case. However, in the initial stage of the oxidation, competition for O₂ will favour formation of MnO over FeO because of the higher heat of formation of the MnO.⁸ A significant increase of the magnetic moment of the sample (up to 30% after the heat

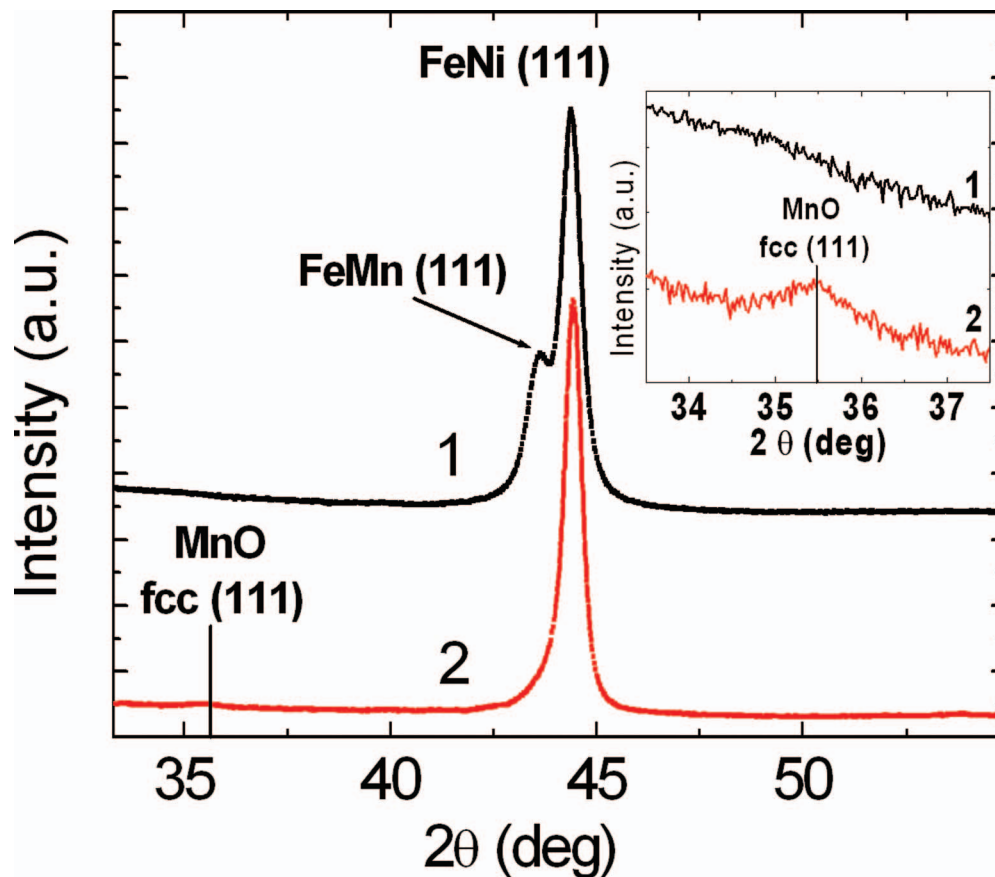


FIG. 3. XRD diffraction patterns of type II sample on the as-deposited state (1) and after annealing at 300 °C (5 min). Inset shows the part of the same graph in a smaller scale.

treatment at 300 °C) speaks in favour of the low degree of oxidation of Fe, if one keeps in mind that magnetization of ferrimagnetic iron oxides is much lower (~ 400 emu/cm³), compared to Fe-rich FeMn phase.

Disappearance of FeMn γ -phase peak does not mean the disappearance of the antiferromagnetic FeMn phase. On the one hand, heat treatment and migration of the Mn atoms can facilitate adjustment of the lattice parameters of FeMn γ -phase to the lattice parameters of FeNi, that leads to a formation of the overlapped diffraction peak, corresponding to FeMn and FeNi lines, as it was observed previously.¹⁹ On the other hand, it is known, that there is not a strong correlation between the amount of the γ -FeMn phase and the exchange bias field H_E .^{11,19}

Noticeable VSM-signal from Fe-rich FeMn phase (let us denote it as f-FeMn) appears to alter the heat treatment at 250 °C. It increases with the annealing temperature, reaches the maximum at 300 °C, and afterwards decreases. Growth of a signal is accompanied by a decrease of the coercivity of the f-FeMn phase. The hysteresis loop of f-FeMn is shifted with respect to zero field, as well as the loop of FeNi layer. Fig. 4(a) shows the loop for type II sample after annealing at 350 °C (10 min), the measurement was done at 180 °C (above the T_b). The FeNi layer is characterized by a narrow loop while the f-FeMn phase shows a wide loop with $H_c \sim 12$ Oe with a slope. Inclination of the loop indicates the volume heterogeneity of f-FeMn phase. It is also possible that the formation of more nucleation centres for magnetic reversal after the oxidation of the FeNi/FeMn interface plays an important role. There exists a small plateau near $|H| = 7$ Oe at which the magnetizations of FeNi and f-FeMn are opposite.

There are detailed and thorough studies of chemical composition throughout the film thickness for FeMn films in the course of gradual oxidation.^{7,8} Based on the results of these studies we can

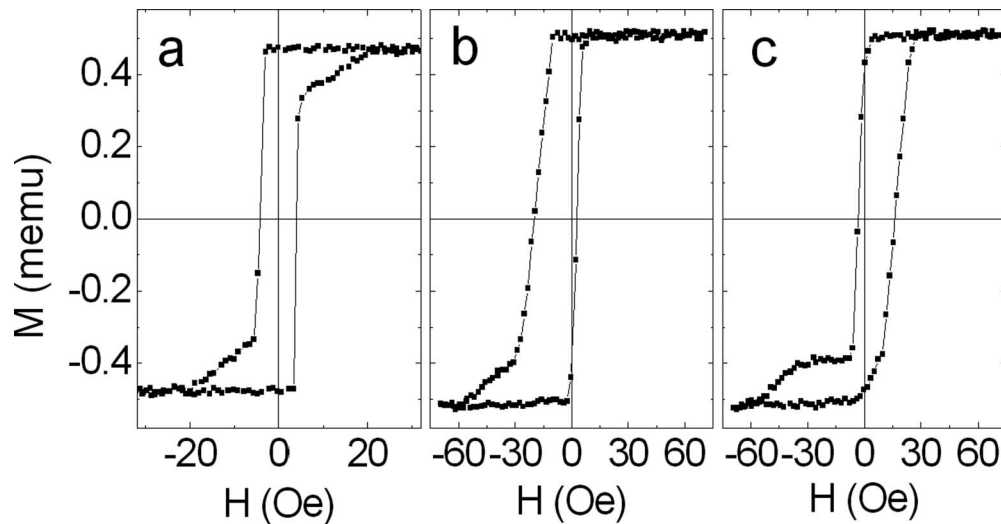


FIG. 4. $M(H)$ loops of the type II sample after annealing at 350°C (10 min): (a) measurements at $T = 180^\circ\text{C}$, (b) measurements at room temperature for field-cooled sample at $H = 300$ Oe, (c) measurements at room temperature for field-cooled sample at $H = -7$ Oe.

assume with a high degree of probability that in our samples the f-FeMn phase begins to form near the surface of the sample, so that the FeNi layer and a layer of f-FeMn are separated by the left FeMn antiferromagnetic layer. The cooling of the sample from 180°C to room temperature, at $H = 300$ Oe, as it is usually done in our work, or at $H = -7$ Oe should lead to different results. In the first case, it is seen that the hysteresis loops of the FeNi and f-FeMn shifted in the same direction (Fig. 4(b)). In the second case, the FeNi and f-FeMn layers acquire exchange bias with opposite anisotropy axis (Fig. 4(c)), because the FeNi and f-FeMn layers were field cooled with their magnetizations in opposite directions. A similar effect was observed for FeNi/FeMn/Co three layered structure.²⁰ Thus, we can conclude that the emerging f-FeMn phase is separated from the FeNi layer by the antiferromagnetic layer. This, however, does not exclude a possible interaction between the two ferromagnetic phases.

Therefore, the cause of change of properties of the FeNi layer is the change of the properties of the adjacent antiferromagnetic FeMn layer and/or interaction between the FeNi and f-FeMn layers through the FeMn layer. Migration of the Mn atoms under the influence of surface oxidation can both change the ratio Fe:Mn in the FeMn layer adjacent to the FeNi, and promote the diffusion of Ni atoms from the FeNi layer to FeMn layer. Both processes contribute to changing the configuration of spins on the interface FeNi/FeMn, which in turn determines the H_E and H_c of the FeNi layer.

Reference data on the effect of an additional ferromagnetic layer are not unambiguous. There is an opinion, that it does not affect the properties of the base (bottom) ferromagnetic layer,²¹ but there are data, supporting its active influence.^{22–24} It can not be ruled out, that under the influence of oxidation not only planar, but also more complex chemical and magnetic structures are formed. Taking into account the enhanced oxidation rate of Mn near the grain boundaries,⁶ and also the columnar structure formation in the films prepared by the magnetron sputtering,^{25,26} we can not exclude the formation of bridges between the ferromagnetic FeNi and f-FeMn layers through the FeMn layer. These issues require further detailed study.

Increase of the annealing time does not make drastic changes in H_c and H_{sw} dependences on the annealing temperature, it shifts their maxima only slightly towards lower temperatures. As a result for an annealing time of 1 h maxima were observed at $T_{ann} \approx 280^\circ\text{C}$, and the maximum values of H_c and H_{sw} were almost unchanged.

As the annealing temperature increases above 300°C , the values of H_c and H_{sw} decrease abruptly (Fig. 2(b)). H_c may decrease due to atomic interdiffusion at the interface between FeNi and FeMn layers.^{14,19} However, the same heat treatment of type I samples leaves magnetic properties of FeNi

layer practically unchanged. Thus, for type II samples, the decrease of H_c can be related to the decrease of the effective thickness of the antiferromagnetic FeMn layer.^{27,28} Changes in the FeMn layer parameters can also cause a change in the regime of coercive behaviour. In some cases the losses on sweeping out a hysteresis loop are primarily in the FeNi layer. In other cases they are confined to the FeNi layer.²⁹ The decrease of H_E for thin enough AFM layers can be caused by several connected factors.⁵ The high temperature annealing results in the change of the hysteresis loops shape which become flatter (Fig. 1(b)). This leads to the H_{sw} reduction.

IV. CONCLUDING REMARKS

In conclusion, heat treatment and partial oxidation of FeMn layer are effective for tuning H_E and H_{sw} parameters in exchange biased FeNi/FeMn bilayers. Low temperature annealing ($T_{ann} < 200^\circ\text{C}$) decreases H_E , that can be useful, for example, for the increase of the magnetic field detectors' sensitivity.^{30,31} Partial oxidation of FeMn layer by the controlled heating in the oxygen containing atmosphere may lead to a significant increase of the H_{sw} of FeNi layer. Fabrication process of the microelectronic devices includes heating and causes the H_E decrease. Therefore, an additional post-fabrication treatment for FeMn partial oxidation can be useful for recovering of the high H_{sw} value. Controlled changes of the thickness of FeMn layer will provide additional opportunities for varying of the value of the annealing temperature and annealing time to reach the maximum switching field parameters.

ACKNOWLEDGMENTS

This work was supported by Russian Ministry of Education and Science, (contract No 02.G36.31.0004), SAIOTEK S-PE12UN025 and REMASEN grants of UPV-EHU, Spanish Government grant MAT2011-27573-C04 and Basque Government "Emergency Research Groups" grants.

- ¹ B. Dieny, "Spin valves," In *Magnetoelectronics*, Ed. M. Johnson (Elsevier, Amsterdam, 2004), p. 67 (396).
- ² U. Hartman, Ed., "Magnetic Multilayers and Giant Magnetoresistance," *Fundamentals and Industrial Applications* (Springer-Verlag, Berlin, 2000), p. 320.
- ³ W. Clemens, H. A. M. van den Berg, G. Rupp, W. Schelter, M. Vieth, J. Wecker, *J. Appl. Phys.* **81**, 4310 (1997).
- ⁴ A. V. Svalov, P. A. Savin, G. V. Kurlyandskaya, J. Gutiérrez, J. M. Barandiarán, and V. O. Vas'kovskiy, *IEEE Trans. Magn.* **38**, 2782 (2002).
- ⁵ J. Nogues and I. K. Schuller, *J. Magn. Magn. Mater.* **192**, 203 (1999).
- ⁶ M. Koguchi, H. Kakibayashi, R. Nakatani, *Jpn. J. Appl. Phys.* **32**, 4814 (1993).
- ⁷ H. Lefakis, T. C. Huang, and P. Alexopoulos, *J. Appl. Phys.* **64**, 5667 (1988).
- ⁸ S. L. Cohen, M. A. Russak, J. M. Baker, T. R. McGuire, G. J. Scilla, S. M. Rossnagel, *J. Vac. Sci. Technol. A* **6**, 918 (1988).
- ⁹ J. M. Daughton, *J. Appl. Phys.* **81**, 3758 (1997).
- ¹⁰ S. Tehrani, J. M. Slaughter, E. Chen, M. Durlam, J. Shi, and M. Deherrera, *IEEE Trans. Magn.* **35**, 2814 (1999).
- ¹¹ E. Gapihan, R. C. Sousa, J. Herault, C. Papusoi, M. T. Delaye, B. Dieny, I. L. Prejbeanu, C. Ducruet, C. Portemont, C. Mackay, and J.-P. Nozieres, *IEEE Trans. Magn.* **46**, 2486 (2010).
- ¹² A. Choukh, *IEEE Trans. Magn.* **33**, 3676 (1997).
- ¹³ K.-Y. Kim, H.-C. Choi, C.-Y. You, and J.-S. Lee, *J. Magn.* **13**, 97 (2008).
- ¹⁴ M. Xu, Z. Lu, T. Yang, C. Liu, S. Cui, Z. Mai, W. Lai, Q. Jia, and W. Zheng, *J. Appl. Phys.* **92**, 2052 (2002).
- ¹⁵ K.-Y. Kim, H.-C. Choi, J.-H. Shim, D.-H. Kim, C.-Y. You, and J.-S. Lee, *IEEE Trans. Magn.*, **45**, 2766 (2009).
- ¹⁶ V. Ng, F. H. Chen, A. O. Adeyeye, *J. Magn. Magn. Mater.* **260**, 53 (2003).
- ¹⁷ K.-Y. Kim, H.-C. Choi, C.-Y. You, and J.-S. Lee, *J. Appl. Phys.* **105**, 07D715 (2009).
- ¹⁸ J. H. Lee, S. J. Kim, C. S. Yoon, C. K. Kim, B. G. Park, and T. D. Lee, *J. Appl. Phys.* **92**, 6241 (2002).
- ¹⁹ K.-C. Chen, Y. H. Wu, K.-M. Wu, L. Horng, and S. L. Young, *J. Appl. Phys.* **101**, 09E516 (2007).
- ²⁰ F. Y. Yang and C. L. Chien, *Phys. Rev. Lett.* **85**, 2597 (2000).
- ²¹ M. G. Blamire, M. Ali, C.-W. Leung, C. H. Marrows, and B. J. Hickey, *Phys. Rev. Lett.* **98**, 217202 (2007).
- ²² S. M. Yoon, J. J. Lim, Y. W. Lee, V. K. Sankaranarayanan, C. G. Kim, and C. O. Kim, *Phys. stat. sol. (a)* **201**, 1680 (2004).
- ²³ V. K. Sankaranarayanan, S. M. Yoon, D. Y. Kim, C. O. Kim, and C. G. Kim, *J. Appl. Phys.* **96**, 7428 (2004).
- ²⁴ D. N. H. Nam, W. Chen, K. G. West, D. M. Kirkwood, J. Lu, and S. A. Wolf, *Appl. Phys. Lett.* **93**, 152504 (2008).
- ²⁵ N. Amos, R. Fernandez, R. Ikkawi, B. Lee, A. Lavrenov, A. Krichevsky, D. Litvinov, and S. Khizroev, *J. Appl. Phys.* **103**, 07E732 (2008).
- ²⁶ A. V. Svalov, E. Fernandez, A. Garcia-Arribas, J. Alonso, M. L. Fdez-Gubieda, and G. V. Kurlyandskaya, *Appl. Phys. Lett.* **100**, 162410 (2012).
- ²⁷ H. Lu, J. F. Bi, K. L. Teo, T. Liew, and T. C. Chong, *J. Appl. Phys.* **107**, 09D717 (2010).

- ²⁸ J. F. Ding, Y. F. Tian, W. J. Hu, W. N. Lin, and T. Wu, [Appl. Phys. Lett.](#) **102**, 032401 (2013).
- ²⁹ M. S. Lund, W. A. A. Macedo, Kai Liu, J. Nogués, Ivan K. Schuller, and C. Leighton, [Phys. Rev. B](#) **66**, 054422 (2002).
- ³⁰ S. T. Halloran, F. C. S. da Silva, H. Z. Fardi, and D. P. Pappas, [J. Appl. Phys.](#) **102**, 033904 (2007).
- ³¹ T. Q. Hung, S. Oh, B. Sinha, J.-R. Jeong, D.-Y. Kim, and Ch. Kim, [J. Appl. Phys.](#) **107**, 09E715 (2010).